INTERNATIONAL JOURNAL OF
COASTAL & OFFSHORE ENGINEERING
IJCOE Vol.2/No. 2/Summer 2018 (1-9)

Available online at: http://ijcoe.org/browse.php?a_code=A-10-117-2&sid=1&slc_lang=en

Effect of FRP Material Properties on Chord SCFs of an FRP-Strengthened Offshore Tubular T-Joint under Brace Axial Loading

Alireza Sadat Hosseini[1*], Mohammad Lesani[2], Mohammad Reza Bahaari

[1] PhD Student, University of Tehran, Tehran, Iran; a.sadat@ut.ac.ir*
[2] Assistant Professor, Sadra University, Tehran, Iran; m.lesani@sadra.ac.ir
[3] Professor, University of Tehran, Tehran, Iran; mbahari@ut.ac.ir

ARTICLE INFO

Article History:
Received: 30 Apr. 2018
Accepted : 1 Sep. 2018

Keywords:
Tubular T-joint
Offshore Platforms
FRP-strengthening
SCF
Finite Element Analysis

ABSTRACT

The relative stress concentration factors (SCF) on the chord member of a tubular T-joint strengthened with FRP which is subjected to brace axial loading are studied. ABAQUS Finite Element software package is used to perform the numerical analyses. Prior to the main studies, the unstiffened joint was validated against the API and Lloyd's Register equations together with the experimental data. Six different types of FRP materials such as Glass/Vinyl ester, Glass/Epoxy (Scotch ply 1002), S-Glass/Epoxy, Aramid/Epoxy (Kevlar 49/Epoxy), Carbon/Epoxy (T300-5208) and Carbon/Epoxy (AS/3501) are used as strengthening material in order to enhance the fatigue life of tubular T-joints through lowering the SCFs. Promising results derived from analyses which show that FRP strengthening method can be considered as an effective method for decreasing the SCF values at tubular T-joints. Results of the analyses for 6mm CFRP layup revealed that under the action of axial loading the FRP strengthening could decrease the SCFs up to 30% and 50% at crown and saddle points of the chord member.

1. Introduction

Offshore jacket platforms are often made of steel circular hollow sections (CHSs) due to high buoyancy and lower drag coefficients and also their adequate structural performance against buckling, bending and torsion. These members are widely used for load-bearing purposes [1]. The most common and basic CHS joint configuration is the T-shape joint which is made by connecting one tube (Brace) perpendicular to the undisturbed exterior surface of the other tube (Chord) using butt welding technique.

Wave loading on offshore structures apply cyclic forces which make them susceptible to fatigue damage Thus, fatigue life prediction in offshore structural joints is necessary to ensure structural safety. Normally, stress-life (S-N) curves are used to assess the fatigue life of offshore structures. In this way, the number of loading cycles that the structure can sustain before fatigue failure could be estimated by hot-spot stress range (HSSR). HSSR is calculated from the stress concentration factor (SCF). According to API [2] part 8.3.1, "for each tubular joint configuration and each type of Brace loading, SCF is defined as: SCF = the hot spot stress range (HSSR)/nominal Brace stress range". In this study, the focus is on the estimation of SCFs at Chord member. Thus, the HSSR is the hot spot stress range on the Chord which must be divided by the nominal direct stress in the Brace member to give the SCF. .

In order to determine the hot-spot stress (HSS) API (2014) presented a conventional method in which, extrapolated geometric stress at the weld toe is to sum the products of the nominal stresses due to each load type and the corresponding SCFs. Estimation of SCFs in tubular as well as non-tubular joints has been the subject of so many numbers of researches since the 1970s. The main objective of these studies was deriving parametric equations. Here, some studies in this field are reviewed.

SCFs could be considered in uni-planar as well as multi-planar joints. Kuang et al. [3] presented parametric equations for estimation of SCF in T, Y, K and KT-joints, using shell elements in a finite element program. It is worth noting that Kuang equations are still widely used in the fatigue design of offshore tubular joints. Equations for SCF estimation in T, Y and X-joints under axial force, in-plane and out-of-plane bending moments were given by Wordsworth and Smedley [4]. Efthymiou and Durkin [5] presented a complete set of SCF equations for T, Y and K-joints.

A wide range of joint geometries under axial loading, in-plane bending and out-of plane bending moments were covered by Hellier et al. [6] finite-element analyses. They presented semi-empirical equations for SCF calculation in tubular T- and Y-joints. Parametric equations were presented by Lloyd's register (LR) [7] which were derived from fitting curves on the existing SCF database. SCFs in Saddle and Crown points of T, Y, X, K and KT-joints are covered in these equations. This is now considered as one of the most liable references for SCF estimation. Chang and Dover [8,9] presented parametric equations for estimation of stress distribution along the Chord-Brace intersection for T, Y, X and KT-joints. SCF equations in multi-planar welded tubular DT-joints were presented by Karamanos et al. [10]. Lotfollahi-yaghin and Ahmadi [11] and Ahmadi et al. [12] proposed equations to predict the SCF along the weld toe of uni-planar KT and multi-plannar DKT-joints under axial loading. SCF distribution parametric equations along the weld toe of outer-inclined and central-vertical Braces of two-planar DKT-joints are presented recently [13, 14]. There are many external strengthening methods for enhancing the mechanical properties of steel members. As a method of strengthening, there are metallic-based methods to decrease the SCFs in CHS joints. Some of these strengthening techniques are reviewed by Lesani et al. [15]. Ramachandra et al. [16] presented formulae for the effect of geometric parameters on SCFs in ring stiffened T and Y-joints.. Nwosu et al. [17] studied the stress distribution along the ring stiffened T-joints through analyzing the effect of geometry, location and number of stiffeners. SCF distributions along the intersections of a T-joint reinforced with doubler plate subjected to the action of combined loadings was investigated by Hoon et al. [18]. Myers et al. [19] studied the effect of three kinds of longitudinal stiffeners in the Chord member on SCF values in jack-up platforms. Fatigue design equations for internal ring-stiffened KT-joints under axial loading were proposed recently [20, 21].

Along with the metallic methods, there are non-metallic external reinforcement methods such as FRP strengthening technique. FRP wrapping method in comparison to the metallic methods is more convenient for handling and application. It resists longer in corrosive areas. Moreover, its potentially high overall durability, light weight, superior strength-to-weight ratio, tailorability and high specific performance attributes make it to be easier for application in areas which conventional materials may encounter deficiencies.

As some examples researches done by Hollaway and Cadei [22], Zhao and Zhang [23] and Zhao [24] on FRP strengthened steel structures are remarkable. Jiao and Zhao [25] studied the - CHSs strengthened with four layers of CFRP under the action of tension loading. Steel short columns strengthened with CFRP were investigated by Shaat and Fam [26] through experiments. Zhao et al. [27] studied the load-bearing capacity of RHSs strengthened with CFRP sheets. Thin walled steel sections which were strengthened with cross-ply FRPs were investigated by Bambach et al. [28]. Wang et al. [29] studied the restraining effect of using external GFRP composites for steel tubes subjected to significant axial displacement. Nishino and Furukawa [30] studied the buckling behavior of CFRP strengthened steel tubes. According to this study, the amount of CFRP used as a strengthening component, has an important impact on delaying buckling and subsequently increasing the section ultimate capacity. The influence of wrapping techniques on deformation capacity of steel tubes under the action of static axial loading was studied by Teng and Hu [31]. Alemdar et al. [32] experimentally and analytically investigated fatigue performance of cover-plate specimens with CFRP reinforced welded connections. A numerical investigation on the failure pattern, ultimate static strength and detailed behavior of GFRP strengthened steel tubular T-joints under axial Brace compressive loading was performed by Lesani et al. [15]. They observed a remarkable increase in joint ultimate capacity due to the combined action of steel and composite against the compressive load. In addition, critical deformations and ovalization of Chord member showed a descending trend up to 50% of the un-strengthened joint. Lesani et al. [33] investigated the ultimate capacity of GFRP strengthened T-joints under the action of static compressive loading through the experiments. Increase up to 50% in the ultimate load-bearing capacity of the tubular joint strengthened by Glass/vinyl ester was observed. Lesani et al. [34] investigated the GFRP strengthened tubular T and Y-joints through a numerical and experimental research program. In this research, the state of the strengthened joint strength, deformation, ovalization, stresses and failure of T and Y-joints under compressive loading were investigated. It was observed that the static strength of tubular T and Y-joints could be improved significantly by the FRP wrapping technique. Chen et al. [35] conducted experiments as well as and numerical analysis to investigate the stress concentration factors in concrete-filled circular chord and square braces in K-joints under balanced axial loading. It is seen that SCFs in concrete-filled circular chord and square braces K-joints were lower than those of corresponding hollow circular chord and square brace K-joints. Yang et al. [36] experimentally studied the SCFs in concrete-filled tubular Y-joints subject to in-plane bending moment. They observed that this strengthening method could effectively reduce the SCF values. Moreover, SCF is evenly distributed when the value of the axial compression ratio in the chord is increased. Jiang et al. [37] experimentally investigated the mechanical behavior

of tubular T-joints reinforced with the grouted sleeve. The failure mode, ultimate load, initial stiffness and deformability of these joint specimens were studied in detail. It was found that the grouted sleeve enhances the strength up to 154.3%~172.7% of the corresponding un-reinforced joint.

According to the literature, during the past years, considerable effort has been devoted to studying SCFs in various unstiffened joints but much fewer on stiffened joints. Metallic-based schemes were mostly used as the strengthening technique. Due to the numerous advantages of non-metallic schemes such as the FRP-wrapping technique on enhancing the static load-bearing capacity of CHSs and prospect of the increasing interest in using such reinforcing schemes, studying the SCFs in FRP-strengthened tubular joints seems to be necessary in order to confirm the efficacy of this method. Sadat Hosseini et al. [38] comprehensively investigated the SCF distribution in FRP-strengthened tubular T-joints under brace axial loading. In this study three types of FRP materials are studied. Moreover, Sadat Hosseini et al. [39] investigated the SCFs in FRP strengthened tubular T-joints subjected to brace axial loading, in-plane and out-of-plane bending moments using finite element analyses. Three FRP materials where used and remarkable results were observed for 1 mm thick strengthening. The present research is aimed at such investigations, in which the results of numerical analyses on 48 steel tubular T-joints strengthened with six various 6mm thick FRP materials were used to deeply investigate the effects of FRP material on the SCF values at the weld toe under Brace axial load. The finite element model was verified against the experimental results extracted from HSE OTH 354 report [7] and the predictions of Lloyd's register (LR) and API equations.

2. Unstiffened Joint FE Model Verification

Here, finite element model of the unstiffened joint was developed and analyses were carried out using ABAQUS [40] software package. The unstiffened T-joint is the joint 1.3 from JISSP project experimental results [7]. Table 1 gives the geometric parameters of the joint.

Table 1. Values of the chord diameter and the other geometric parameters of the T-joint

Reference	D (mm)	α $=2L/D$	β $=d/D$	γ $=D/2T$	τ $=t/T$
JISSP joint 1.3	508	10	0.8	20.3	0.99

The finite element geometries of the unstiffened joints are exactly as same as the geometry of the experimental models. In this study, ABAQUS 3D brick elements (C3D20) are incorporated to model the unstiffened joint geometry. This type of element is defined by 20 nodes having three degrees of freedom per node.

Fig. 1(a) illustrates the isometric view of the T-joint numerical model. The mesh enlargement view of the T-joints is presented in Fig. 1(b). Moreover, the weld profile at the Brace-Chord intersection is modeled in order to achieve accurate stresses along the Chord-Brace intersection. It is important to model the weld geometry with accurate dimensions. Here, the weld profile along the Brace-Chord intersection satisfies the specifications addressed in AWS [41]. Along with the AWS (2010) specifications some simplifications according to the techniques utilized by Lee [42] and Chiew et al. [43] are used to make it possible to create a smooth and adequately accurate weld profile. For further discussion, the reader is referred to Lie et al. [44]. In Fig. 1(c) the weld profile section in finite element model can be seen. Weld profile is modeled as a sharp notch by using 3D brick 20 nodes elements. The weld material properties are assumed the same as the Chord and Brace.

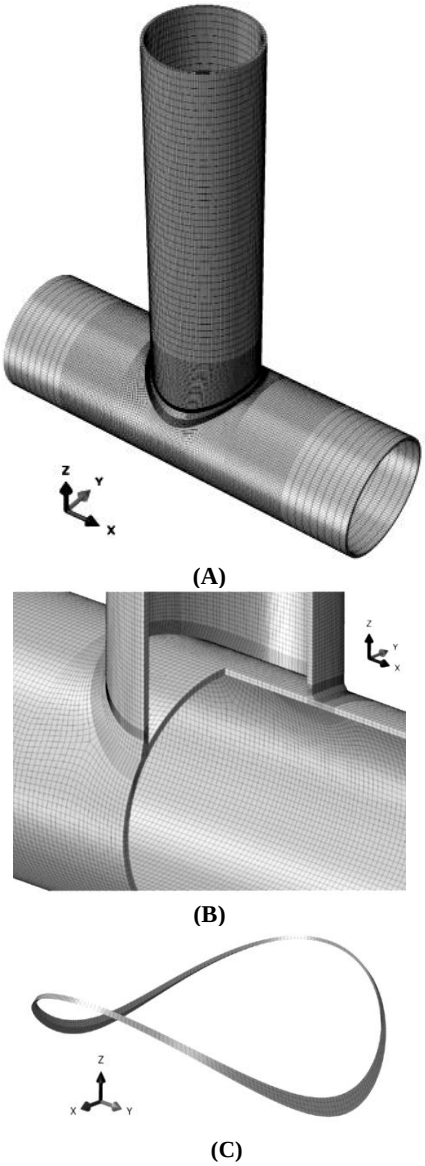

Figure 1. The mesh generated for the t-joint (JISSP joint 1.3) using the sub-zone method; (a): Isometric view, (b): Mesh enlargement, (c): 3d view of the weld profile

Different sub-zone mesh generation methods were used for the weld profile, hot spot stress region, FRP wrapping area and other regions of the joint. The mesh in the hot-spot stress region is much finer than the other zones since more computational precision is required in this area. FRP wrapping areas have coarser meshes but still fine enough to ensure computational accuracy.

The boundary conditions are chosen in such a way to represent the actual boundary conditions of the experiment. Here in the analyses, Chord ends were assumed to be fixed.

In order to determine the stress concentration factors in a tubular joint, a linear elastic numerical analysis needs to be performed [45]. The Young's modulus and Poisson's ratio of steel are taken as 207 GPa and 0.3, respectively exactly as same as the experimental model. In order to estimate the SCFs, the method introduced by IIW-XV-E [46] is implemented. In this method, the peak stress at the weld toe is calculated by linear extrapolation of the von-Mises stresses at distances of 0.4T and 1.4T from the weld toe; where T is the thickness of the Chord member. SCF is calculated by dividing the von Mises stresses at weld toe by the nominal stress on the Brace member. Fig, 2 shows the extrapolation zone on the crown point of the chord member.

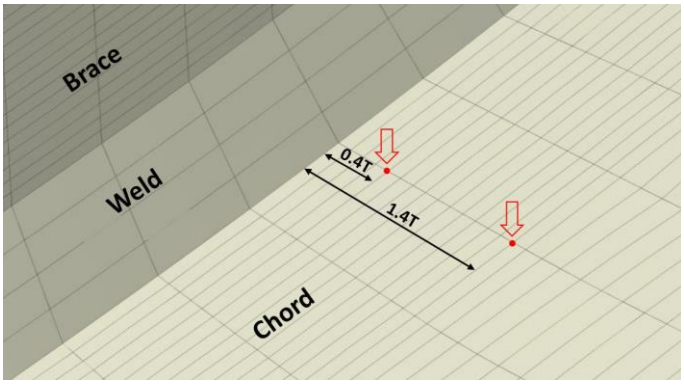

Figure 2. The extrapolation zone on the chord member

In order to validate the finite element model, Lloyd's Register equations and API equations for SCF computation together with the test results published in HSE OTH 354 report for JISSP joint 1.3 [7] is used. Table 2 summarizes the verification results at the Saddle and Crown points. In this table, e1 and e2 show the percentage of relative difference of Lloyd's Register and API equations with test results respectively, and e3 denotes the percentage of the relative difference between the results of finite element model and the experiment results. According to Table 2, it is obvious that the finite element model predicts the SCFs at Crown and Saddle points accurately which is in good agreement with the test results and therefore, the FE model is validated.

Table 2. Comparison of finite element results with experimental data and predictions of LR and API equations

Position	Test	LR Eq.	API Eq.	FEM	e_1	e_2	e_3
Crown	5.4	3.94	3.85	5.3	27	28.7	1.9
Saddle	11.4	10.54	12.13	11.1	7.5	6.4	2.6

3. Stiffened Joint FE Modeling

In the previous section, it is explained how the unstiffened model has been generated and verified against the experimental model. This section gives an account of the specifications of the FRP strengthened numerical model.

FRPs are composed of two distinguishable parts namely fibers and matrix. Thus, various compositions could be made. In this study six types of common FRP materials, Glass/Vinyl ester, Glass/Epoxy (Scotch ply 1002), S-Glass/Epoxy, Aramid/Epoxy (Kevlar 49/Epoxy), Carbon/Epoxy (T300-5208) and Carbon/Epoxy (AS/3501), are used as strengthening material on the T-joint in order to find out how different FRP materials affect the SCF values. Table 3 demonstrates the properties of the FRPs used in the analyses. In this table, subscripts ''1'' and ''2'' stand for the fiber longitudinal and transverse directions respectively.

Table 3. FRP properties [15, 47, 48]

Mechanical properties	E_1 [Gpa]	E_2 [Gpa]	ν_{12}	G_{12} [Gpa]	G_{13} [Gpa]	G_{23} [Gpa]
Glass/ Vinyl ester	28	7	0.29	4.5	4.5	2.54
Glass/Epoxy (Scotch ply 1002)	38.6	8.27	0.26	4.14	4.14	3.1
S-Glass/Epoxy	43	8.9	0.27	4.5	3.18	3.18
Aramid/Epoxy (Kevlar 49/Epoxy)	76	5.5	0.34	2.3	2.3	2.01
Carbon/Epoxy (T300-5208)	132	10.8	0.24	5.7	5.7	3.4
Carbon/Epoxy (AS/3501)	138	8.96	0.3	7.1	7.1	2.82

FRP material is modeled using shell elements defined as a skin layer on the 3D unstiffened joint model. The specifications of the unstiffened joint model are given in the previous section. The FRP shell elements are ABAQUS element type S4R, which is a 4-node doubly curved thin or thick shell with reduced integration. The interior surface of the FRP elements are tied to the external surface of the solid elements of the un-stiffened joint geometry and these two surfaces share the same nodes and mesh topology. This is similar to the actual application of FRP layup on the surfaces. Here a perfect bond state was considered and no cohesive/adhesive element was modeled at the FRP and the steel substrate interface. This is not an irrational assumption since the bond between FRP layer and steel stays undisturbed in the elastic range of

loading according to the experimental and numerical analysis [33]. Fig. 3 shows an enlarged section of the strengthened T-joint.

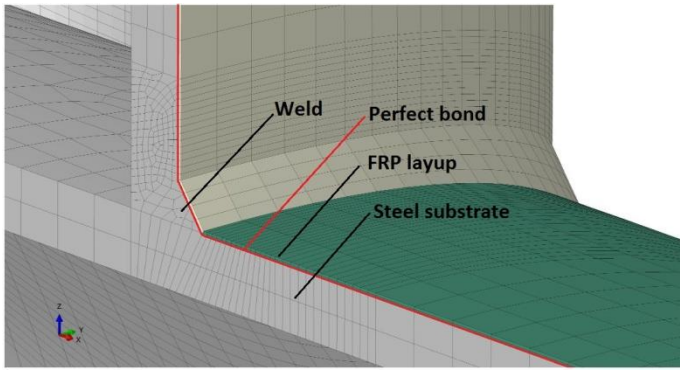

Figure 3. Mesh enlargement around crown point of the numerical model of the frp wrapped t-joint

FRP fibers are considered in two major directions. The 0o (Chord hoop direction and along the Brace longitudinal axis) and 90o orientations. Fig. 4 clarifies how these fiber orientations are being considered in FRP modeling.

For all of the analyses, the strengthening materials are applied on the T-joint having a thickness of 6mm and a wrapping length equal to one diameter of the relative strengthened member (1D on the Chord and 1d on the Brace member).

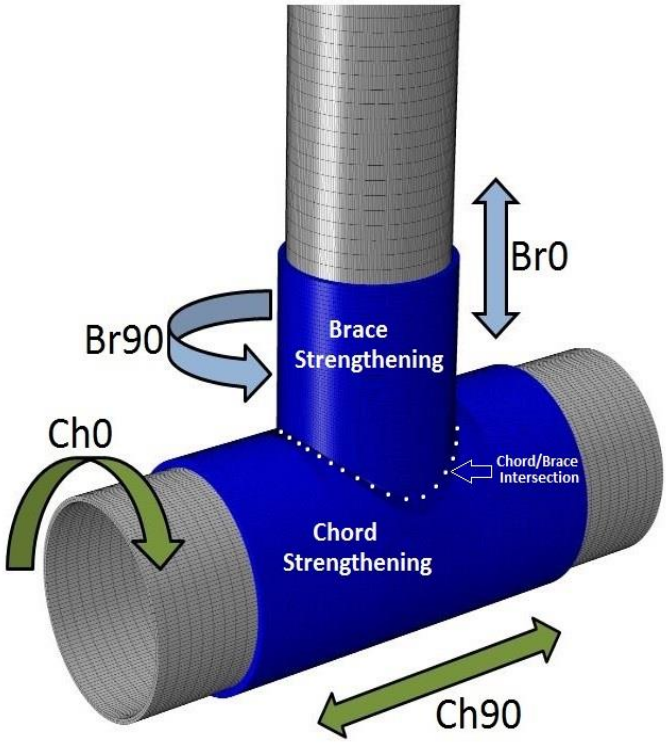

Figure 4. The FRP wrapped T-joint with definition of 0º and 90º fiber orientations in the FRP layup on chord and brace

4. Analysis and Results

Here the results of the analyses on the strengthened T-joints are presented. In order to investigate the stress concentration in FRP strengthened tubular T-joints under Brace axial loading, models were generated and analyzed using ABAQUS finite element software package. The six FRP materials (Glass/Vinyl ester, Glass/Epoxy (Scotch ply 1002), S-Glass/Epoxy, Aramid/Epoxy (Kevlar 49/Epoxy), Carbon/Epoxy (T300-5208) and Carbon/Epoxy (AS/3501)) are applied on the basic joint geometry and the stiffened joints were analyzed. Table 4 gives the abbreviations used for FRP materials in this study. Stresses at Saddle and Crown points at the weld toe on the Chord surface are extracted (HSSR) using IIW-XV-E method and divided by the nominal Brace stress range to find the SCFs at the strengthened joint.

Table 4. The abbreviations of the strengthening schemesand FRP orientations

Abbreviation	Description
Ch0	Chord strengthening with 0º fibers orientation
Ch90	Chord strengthening with 90º fibers orientation
Br0	Brace strengthening with 0º fibers orientation
Br90	Brace strengthening with 90º fibers orientation
Ch0&Br0	Chord and Brace strengthening with 0º fibers orientation on both Chord and Brace
Ch0&Br90	Chord and Brace strengthening with 0º fibers orientation on Chord and 90º fibers orientation on Brace
Ch90&Br0	Chord and Brace strengthening with 90º fibers orientation on Chord and 0º fibers orientation on Brace
Ch90&Br90	Chord and Brace strengthening with 90º fibers orientation on both Chord and Brace

The analyses were carried out in three phases. At first, the Chord alone was strengthened in order to investigate the effects of strengthening the Chord member on SCFs. In the second phase, FRP was applied only to the Brace member to study the Brace strengthening effects, and finally, in the third phase, both of the Chord and Brace members were strengthened. SCF values of the strengthened joints are extracted and divided by the SCFs of the unstiffened joint at Crown and Saddle points to find the SCF ratios. Two major orientations (0o and 90o) are selected for the fibers in FRP layups. Table 5 presents the abbreviations for the strengthening schemes.

Table 5. The abbreviations of the FRP materials

Abbreviation	Description
GV	Glass/vinyl ester
GE	Glass/Epoxy (Scotchply 1002)
SGE	S-glass/Epoxy
AE	Aramid/Epoxy (Kevlar 49/Epoxy)
T300	Carbon/Epoxy (T300-5208)
AS	Carbon/Epoxy (AS/3501)

The results of the analyses of investigation of the effect of using six different FRP compositions as the

strengthening material on the T-joint (JISSP joint 1.3) on SCF values at Crown and Saddle points, when the joint is under Brace axial loading were investigated. The joint is under 10 tones load which is monotonously distributed on the top of the Brace member. Fig. 5 shows the von Mises stress distribution around the Chord/Brace intersection area for the unstrengthened joint as long as the strengthened joint with Carbon/Epoxy (AS/3501) in order to make sense how FRP strengthening could affect the von misses stresses. Stresses at the weld toe in Chord Crown and Saddle points are calculated according to the IIW-XV-E method which is explained previously. These stresses are divided by the nominal stress at the Brace member and thus, SCF values are extracted.

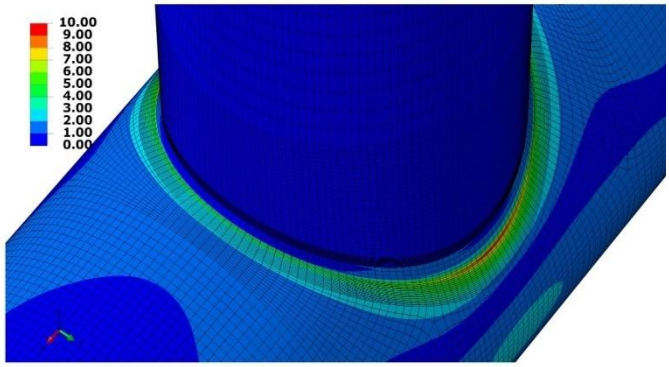

(A)

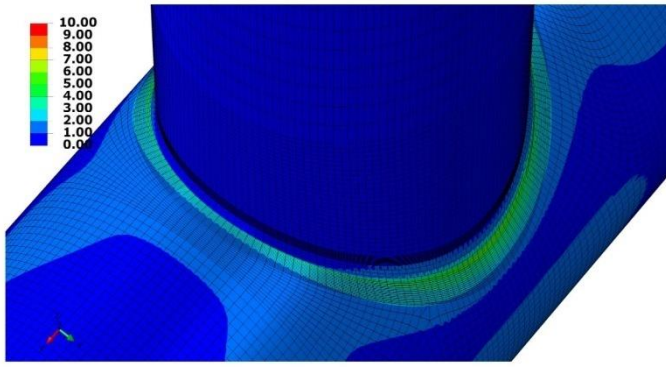

(B)

Figure 5. Von misses stresses on the joint surface for 10 tones axial load at the top of the brace: a) Unstrengthened joint; b) Strengthened joint

Analyses are performed for all fix types of FRPs and results are given for different strengthening schemes. Fig. 6 and Fig. 7 show the relative SCFs (SCF_s: SCF at the strengthened joint divided by SCF_u: SCF at the unstiffened joint) at Crown and Saddle points respectively.

As it can be seen in Fig. 6, the more the stiffer FRP used as strengthening material, the more the SCF values decreases. According to this Figure, fibers orientation on the Chord member has a chronic effect on SCFs. It is seen that the decreasing effect of FRP wrapping on the Chord member when the fibers are in 90º, is three times the FRP wrapping with 0o orientation on average.

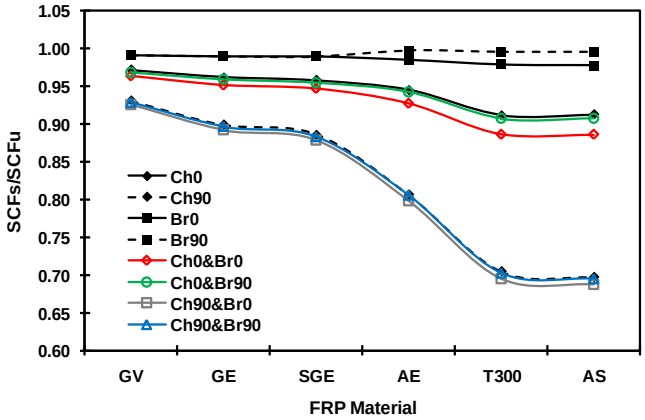

Figure 6. Ratio of SCF at the crown point of the FRP strengthened tubular t-joint with different FRP materials to SCF distribution in un-strengthened joint under brace axial load

According to Fig. 6, in order to further reduce the SCFs at the Crown Point, fibers should be aligned in 90º orientation. Applying FRP only on the Brace member has a negligible unpleasant increasing effect on SCFs (square and dash square lines in Fig. 6). Although Brace strengthening has an undesired effect on SCF, in order to keep the integrity of joint strengthening, in practical applications, both Chord and Brace members will be wrapped.

As an interesting result, applying FRP on both Chord and Brace members simultaneously has more effect on SCF reduction comparing to the other schemes (hollow square and hollow rectangular lines). Given that, using FRP on Brace member, with fibers in 0o orientation has the weakest increasing effect on SCFs, and on the other hand, using FRP with fibers in 90o orientation on the Chord member has the strongest decreasing effect on SCFs, the best layup would be Ch90&Br0. Focus on the effect of FRP material reveals that using Carbon/Epoxy (AS/3501) with 6mm thickness on both Chord and Brace members decreases the SCFs by 30 percent at the Crown point. Generally, the decreasing effect of using stiffer FRPs such as CFRP is about 5 times the GFRP material.

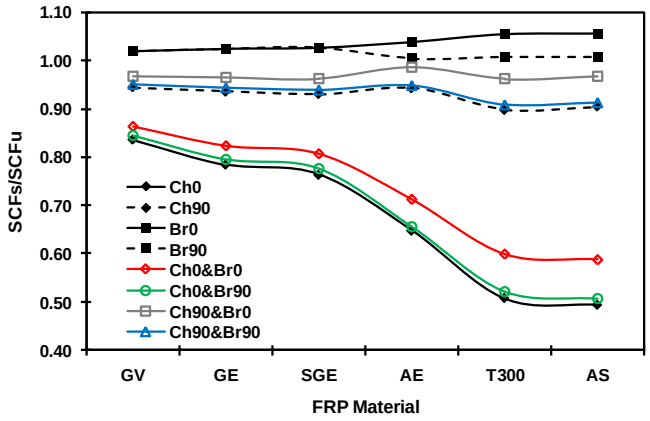

Figure 7. Ratio of SCF at the saddle point of the FRP strengthened tubular T-joint with different FRP materials to SCF distribution in un-strengthened joint under brace axial load

Considering the T-joint when the Chord member is strengthened (Fig. 7), it is seen that, stiffer FRP material (higher mechanical properties) shows more effectiveness in decreasing the SCF values at the Saddle point (Fig. 7). As clearly envisaged from this Figure, using 6mm Carbon/Epoxy material has effectiveness of about three times the GFRP material on SCF reduction, which is about 50% at the Saddle point. As like as the Crown Point, strengthening the Brace member has also an increasing effect on SCFs at the Saddle point. These effects are amplified by increasing the mechanical properties of FRP materials. Between 0^o and 90^o orientations, using 90o orientation has a weaker additive effect on SCFs. The adverse effect of using higher modulus FRP materials on the Brace member is about maximum 5% at the Saddle point. The effect of different strengthening FRP materials on SCF values when the Chord and Brace members of the T-joint are simultaneously strengthened is also illustrated in this Figure. Based on this figure, applying 6mm Carbon-epoxy on the Chord member with 0^o fibers orientation and 90^o fibers orientation on the brace is the most effective layup which can lower the SCFs up to 50% at the Saddle point. This confirms the effectiveness of FRP strengthening on SCF reduction in tubular T-joints.
Having Fig. 6 and Fig. 7 along with the mechanical properties given in Table 1, one can find how the change in the value of each mechanical property in two main extreme fiber orientations (0o and 90o) will affect the SCFs under axial loadings.

5. Summary and Conclusions

In this research, changes in SCF values at Crown and Saddle points on the Chord member of the tubular T-joint due to change in FRP material used for wrapping the joint was investigated. The FRP layup thickness is 6mm in all models. The following conclusions were derived from this study:

- Change of fiber and/or matrix material properties corresponds to change in FRP mechanical properties. Use of FRP material with higher values of mechanical properties as the strengthening material shows more effect on SCF values reduction. In general, CFRP strengthening can reduce the SCFs up to 30% and 50% at Crown and Saddle points respectively.
- Among the six common composite material, CFRP materials have the effectiveness of about 3 and 2.5 times the GFRP materials in SCF reduction at Crown and Saddle points respectively.
- According to the results, the most effective schemes under axial loading at Crown and Saddle points are Ch90Br0 and Ch0Br90 (see Table 5) respectively. Besides, in as much as for common practical applications, the joint will completely wrapped with FRP (Chord and Brace are strengthened) the Brace and Chord should be strengthened with FRPs in which the fibers are aligned in both longitudinal and hoop directions.
- Due to the better fatigue performance of CFRP materials in comparison to other composite materials such as GFRP, and based on the findings of this study, it is recommended to use CFRP composites as wrapping and strengthening material for fatigue life extension of tubular joints. Anyway, economical issues must be addressed.

6. References

1- Jia, J., (2008), *An efficient nonlinear dynamic approach for calculating wave induced fatigue damage of offshore structures and its industrial applications for lifetime extension*, Applied Ocean Research, Vol.30, p.189-198.
2- API (American Petroleum Institute), (2014), *Recommended practice for planning, designing and constructing fixed offshore platforms - working stress design*, API RP 2A WSD, 22nd edition.
3- Kuang, J. G., Potvin, A. B., and Leick, R. D., (1975), *Stress concentration in tubular joints*, Proceedings of the offshore technology conference (OTC 2205), Houston, Texas, US.
4- Wordsworth, A. C., and Smedley, G. P., (1978), *Stress concentrations at unstiffened tubular joints*, Proceedings of the European offshore steels research seminar, Paper 31, Cambridge, UK.
5- Efthymiou, M., and Durkin, S., (1985), *Stress concentrations in T/Y and gap/overlap K-joints*, Proceedings of the conference on behavior of offshore structures, Delft, Netherlands.
6- Hellier, A. K., Connolly, M., and Dover, W. D., (1990), *Stress concentration factors for tubular Y and T-joints*, International Journal of Fatigue, Vol.12, p.13-23.

7- Health and Safety Executive (UK), (1997), OTH 354: Stress concentration factors for simple tubular joints - assessment of existing and development of new parametric formulae. Prepared by Lloyd's Register of Shipping.

8- Chang, E., and Dover, W. D., (1999), *Parametric equations to predict stress distributions along the intersection of tubular X and DT-joints*, International Journal of Fatigue, Vol.21, p.619-635.

9- Chang, E., and Dover, W. D., (1999), *Prediction of stress distributions along the intersection of tubular Y and T-joints*, International Journal of Fatigue, Vol.21, p.361-381.

10- Karamanos, S. A., Romeijn, A., and Wardenier, J., (2002), *SCF equations in multi-planar welded tubular DT-joints including bending effects*, Marine Structures, Vol.15, p.157-173.

11- Lotfollahi-Yaghin, M. A., and Ahmadi, H., (2010), *Effect of geometrical parameters on SCF distribution along the weld toe of tubular KT-joints under balanced axial loads*, International Journal of Fatigue, Vol.32, p.703-719.

12- Ahmadi, H., Lotfollahi-Yaghin, M. A., and Aminfar, M. H., (2011), *Geometrical effect on SCF distribution in uniplanar tubular DKT- joints under axial loads*, Journal of Constructional Steel Research, 67, p.1282-1291.

13- Lotfollahi-Yaghin, M. A., and Ahmadi, H., (2011), *Geometric stress distribution along the weld toe of the outer Brace in two planar tubular DKT-joints: parametric study and deriving the SCF design equations*, Marine Structures, Vol.24, p.239-260.

14- Ahmadi, H., Lotfollahi-Yaghin, M. A., and Aminfar, M. H., (2011), *Distribution of weld toe stress concentration factors on the central Brace in two-planar CHS DKT connections of steel offshore structures*, Thin-Walled Structures, Vol.49, p.1225-1236.

15- Lesani, M, Bahaari, M. R., and Shokrieh, M. M., (2013), *Numerical investigation of FRP-strengthened tubular T-joints under axial compressive loads*, Composite Structures, Vol.100, p.71-78.

16- Ramachandra Murthy, D. S., Madhava Rao, A. G., Ghandi, P., and Pant, P.K., (1992), *Structural efficiency of internally ring stiffened steel tubular joints*, Journal of Structural Engineering, Vol.118, p.3016-3035.

17- Nwosu, D. I., Swamidas, A. S. J., and Munaswamy, K., (1995), Numerical stress analysis of internal ring-stiffened tubular T joints, Journal of Offshore Mechanics and Arctic Engineering, Vol.117, p.113-125.

18- Hoon, K. H., Wong, L. K., and Soh, A. K., (2001), *Experimental investigation of a doubler-plate reinforced tubular T-joint subjected to combined loadings*, Journal of Constructional Steel Research, Vol.57(9), p.1015-1039.

19- Myers, P. T., Brennan, F. P., and Dover, W. D., (2001), *The effect of rack/rib plate on the stress concentration factors in jack up Chords*, Marine Structures, Vol.14, p.485-505.

20- Ahmadi, H., Lotfollahi-Yaghin, M. A., Shao, Y. B., and Aminfar, M. H., (2012), *Parametric study and formulation of outer Brace geometric stress concentration factors in internally ring stiffened tubular KT-joints of offshore structures*, Applied Ocean Research, Vol.38, p.74-91.

21- Ahmadi, H., Lotfollahi-Yaghin, M. A., and Shao, Y. B., (2013*), Chord-side SCF Distribution of central Brace in internally ring stiffened tubular KT-joints: A geometrically parametric study*, Thin-Walled Structures, Vol.70, p.93-105.

22- Hollaway, L. C., and Cadei, J., (2002), *Progress in the technique of upgrading metallic structures with advanced polymer composites*, Progress in Structural Engineering and Materials, Vol.4(2), p.131-148.

23- Zhao, X. L., and Zhang, L., (2007), *State of the art review on FRP strengthened steel structures*, Engineering Structures, Vol.29(8), p.1808-1823.

24- Zhao, X. L., (2009), *FRP strengthened metallic structures*, Thin Walled Structures, Special Issue, Vol.47(10), p.1019.

25- Jiao, H., Zhao, and X. L., (2004), *CFRP strengthened butt welded very high strength (VHS) circular steel tubes*, Thin- Walled Structures, Vol.42(7), p.963-978.

26- Shaat, A., and Fam, A., (2007), *Finite element analysis of slender HSS columns strengthened with high modulus composites*, Steel and Composite Structures, Vol.7(1), p.19-34.

27- Zhao, X. L., Fernando D., and Al-Mahaidi R., (2006), *CFRP strengthened RHS subjected to transverse end bearing force, Engineering Structures*, Vol.28(11), p.1555-1565.

28- Bambach, M. R., Jama, H. H., and Elchalakani, M., (2009), *Axial capacity and design of thin walled steel SHS strengthened with CFRP*, Thin-Walled Structures, Vol.7(10), p.1112-1121.

29- Wang, X. G., Bloch, J. A., and Cesari, D., (1991), *Axial crushing of tubes made of multi-materials*, Proceedings of the 4th international MECAMAT seminar on mechanics and mechanisms of damage in composites and multi-materials, St. Etienne, France, London, Mechanical Engineering Publications Ltd., p.351-360.

30- Nishino, T., and Furukawa, T., (2004), *Strength deformation capacities of circular hollow section steel member reinforced with carbon fiber*, Proceedings of the 7th pacific structural steel conference, Long Beach, California, USA, American Institute of Steel Construction.

31- Teng, J. G., and Hu, Y. M., (2007), *Behaviour of FRP jacketed circular steel tubes and cylindrical shells under axial compression*, Construction and Building Materials, Vol.21(4), p.827-838.

32- Alemdar, F., Matamoros, A., Bennett, C., Barrett-Gonzalez, R., and Rolfe, S. T., (2012), *Use of CFRP Overlays to strengthen welded connections under fatigue loading*, Journal of Bridge Engineering, Vol.17(3), p.420-431.

33- Lesani, M, Bahaari, M. R., and Shokrieh, M. M., (2014), *Experimental investigation of FRP-strengthened tubular T-joints under axial compressive loads*, Construction and Building Materials, Vol.53, p.243-252.

34- Lesani, M., Bahaari, M. R., and Shokrieh, M. M., (2015), *FRP wrapping for the rehabilitation of Circular Hollow Section (CHS) tubular steel connections*, Thin-Walled Structures, Vol.90, p.216-234.

35- Chen, Y., Hu, K., and Yang, J., (2016), *Investigation on SCFs of concrete-filled circular Chord and square Braces K-joints under balanced axial loading*, Steel and Composite Structures, Vol.21(6), p.1227-1250.

36- Yang, J., Yang, C., Su, M., and Lian, M., (2016), *Stress concentration factors test of reinforced concrete-filled tubular Y joints under in-plane bending*, *Steel and Composite Structures*, Vol.22(1), p.203-216.

37- Jiang, S., Guo, X., Xiong, Z., Cai, Y., and Zhu, S., (2017), *Experimental studies on behavior of tubular T-joints reinforced with grouted sleeve*, Steel and Composite Structures, Vol.23(5), p.585-596.

38- Sadat Hosseini, A., Bahaari, M. R., Lesani, M., (2018), *SCF distribution in FRP-strengthened tubular T-joints under brace axial loading*, Scientia Iranica, Articles in Press, Accepted Manuscript, Available Online from 06 May 2018.

39- Sadat Hosseini, A., Bahaari, M. R., Lesani, M., (2017), *SCF in FRP strengthened tubular T-joints under brace axial loading, in-plane bending and out-of-plane bending moments*, Proceedings of the 4th conference on smart monitoring, assessment and rehabilitation of civil structures, Zurich, Switzerland, Paper no. 151.

40- ABAQUS/CAE, (2014), Standard user's manual, Version 6.14-1.

41- AWS (American Welding Society), (2010), *Structural welding code, AWS D 1.1:2010* (22nd Edition). Miami, FL (USA), American Welding Society, Inc.

42- Lee, M. M. K., (1999), *Estimation of stress concentrations in single-sided welds in offshore tubular joints*, International Journal of Fatigue, Vol.21, p.895-908.

43- Chiew, S. P., Soh, C. K., Fung, T. C., and Soh, A. K., (1999), *Numerical study of multi-planar tubular DX-joints subject to axial loads*, Computers and Structures, Vol.72, p.746-761.

44- Lie, S. T., Lee, C. K., and Wong, S. M., (2001), *Modeling and mesh generation of weld profile in tubular Y-joint*, Journal of Constructional Steel Research, Vol.57, p.547-567.

45- N'Diaye, A., Hariri, S., Pluvinage, G., and Azari, Z., (2007), *Stress concentration factor analysis for notched welded tubular T joints*, International Journal of Fatigue, Vol.29, p.1554-1570.

46- IIW-XV-E., (1999), International institute of welding subcommission XV-E, *recommended fatigue design procedure for welded hollow section joints*, IIW Docs, XV-1035-99/XIII-1804 99, International Institute of Welding, France.

47- Ganesh, K, and Naik, N. K., (2005), *Some strength studies on FRP laminates*, Journal of Composite Structures, Vol.24, p.51-58.

48- Kollár, L. P., and Springer, G. S., (2003), *Mechanics of composite structures*, Cambridge university press.